PROTEINS: Structure, Function, and Genetics 49:378–384 (2002)

Investigating the Ultrastructure of Fibrous Long Spacing Collagen by Parallel Atomic Force and Transmission Electron Microscopy

Alvin C. Lin and M. Cynthia Goh*
Department of Chemistry, University of Toronto, Toronto, Ontario, Canada

ABSTRACT **The ultrastructure of fibrous long spacing (FLS) collagen fibrils has been investigated by performing both atomic force microscopy (AFM) and transmission electron microscopy (TEM) on exactly the same area of FLS collagen fibril samples. These FLS collagen fibrils were formed in vitro from type I collagen and α_1-acid glycoprotein (AAG) solutions. On the basis of the correlated AFM and TEM images obtained before and after negative staining, the periodic dark bands observed in TEM images along the longitudinal axis of the FLS collagen fibril correspond directly to periodic protrusions seen by AFM. This observation is in agreement with the original surmise made by Gross, Highberger, and Schmitt (Gross J, Highberger JH, Schmitt FO, Proc Natl Acad Sci USA 1954;40:679-688) that the major repeating dark bands of FLS collagen fibrils observed under TEM are thick relative to the interband region. Although these results do not refute the idea of negative stain penetration into gap regions proposed by Hodge and Petruska (Petruska JA, Hodge AJ. Aspects of protein structure. Ramachandran GN, editor. New York: Academic Press; 1963. p. 289–300), there is no need to invoke the presence of gap regions to explain the periodic dark bands observed in TEM images of FLS collagen fibrils. Proteins 2002;49:378–384.**

Key words: AFM; TEM; energy dispersive X-ray spectroscopy; sample holder; FLS collagen; collagen fibril structure; negative staining

INTRODUCTION

Collagen is the most abundant structural protein in mammalian tissues. It is present in bone, cartilage, skin, teeth, and tendon and is used as a biomaterial in a variety of industrial applications.[1] The basic rodlike unit, the collagen monomer, is ~300 nm long and 1.5 nm in diameter. Although collagen monomers typically form native-type fibrils characterized by the presence of a ~67-nm banding periodicity, they can also assemble into other structures. In particular, fibrous long spacing (FLS) collagen fibrils, which are characterized by banding periodicity larger than 67 nm, can be formed in vitro [e.g., by the addition of α_1-acid glycoprotein (AAG)][2,3] and have been found in vivo associated with a number of pathological conditions: atherosclerotic plaques,[4] Hodgkin's disease,[5] myeloproliferative disorder,[6] and silicosis.[7]

Electron micrographs have provided the most information in understanding the ultrastructure of collagen fibrils.[8,9] Based on images obtained by transmission electron microscopy (TEM), collagen monomers are proposed to align parallel to the main axis of the fibril arranged in a staggered manner.[10] In negatively stained TEM images of collagen fibrils, the banding pattern is ascribed to stain penetration and deposition into vacant spaces between monomers, and thus, the periodic dark bands along these fibrils are commonly referred to as "gap" regions or zones. Lighter bands would correspond to "overlap" zones where negative stain is not able to penetrate. This scheme of "gap" and "overlap" zones along the fibril is generally known as the Hodge-Petruska model.[10,11] Although derived from native-type collagen fibrils, this idea of negative stain penetration into gap regions has also been invoked to explain the dark banding staining patterns observed in TEM images of FLS collagen fibrils.[12] For native-type collagen formed in vitro and FLS collagen fibrils formed in vitro from type I collagen and AAG, the banding periodicities of alternating dark and light bands have been shown to be ~67 nm and ~270 nm respectively.[8,11,13–15]

Within the last decade, the same measured periodicities for native-type collagen[16–19] and FLS collagen fibrils formed in vitro from type I collagen and AAG[3,20,21] have also been observed by atomic force microscopy (AFM). In the AFM images, the observed banding is due to topography, with trenches or protrusions spaced every ~67 nm and ~270 nm for native-type collagen and FLS collagen fibrils, respectively. However, the relationship between these topographical features elucidated by AFM and the banding patterns of negatively stained fibrils observed in TEM images is not clear. Although the Hodge-Petruska model would infer the presence of gap zones in the regions corresponding to the TEM dark bands, Gross et al.,[2] in their original work on FLS collagen fibrils formed in vitro from type I collagen and AAG, suggested that "the major repeating dark bands of the FLS may be thick relative to the interband region." Performing both AFM and TEM on

*Correspondence to: Dr. M. C. Goh, Department of Chemistry, University of Toronto, Toronto, Ontario, Canada, M5S 3H6. E-mail: cgoh@chem.utoronto.ca

Received 15 May 2002; Accepted 26 June 2002

exactly the same area of FLS collagen fibril, before and after negative staining, would allow us to investigate this relationship between protrusions observed by AFM and dark bands observed by TEM.

Investigating systems with both AFM and TEM has become increasingly prevalent. For example, both techniques have been used in conjunction to examine a number of different biological systems: collagen fibrils,[22,23] proteins,[24] protein crystals,[25] bacteriophage T4,[26] rat liver sinusoidal endothelial cells,[27] DNA with bacteriophage phi 29 connector,[28] cartilage,[29] polysomes,[30] rat calvaria,[31] and nanotubular structures in pulmonary surfactant.[32] Moreover, the use of both techniques in conjunction is very common in the characterization of polymers, nanostructures, and thin films,[33–39] and in studies of colloids and clusters.[40] However, because each technique requires different sets of imaging conditions, the use of both AFM and TEM on the same sample area has been difficult to achieve, especially for more structurally complex biological samples where staining and other sample preparations are involved. By developing a novel sample holder for carbon-coated indexed TEM grids, we have been able to image *exactly* the same sample area *repetitively* under both AFM and TEM.[21] In this article, we take advantage of this capability to investigate the morphology of FLS collagen fibrils by a parallel AFM and TEM approach.

MATERIALS AND METHODS

In Vitro Preparation of FLS Collagen Fibrils

Preparation of FLS collagen fibrils were analogous to previously described methods.[2,3,13,20] Equal volumes of type I collagen solution (1 mg/mL) with AAG solution (1 mg/mL) were mixed and dialyzed (molecular weight cutoff of 12,000–14,000 kDa) at room temperature overnight to a final pH of ~6.5. The dialyzed sample was a white turbid mixture. The collagen solution (1 mg/mL) was prepared first by dissolving type I collagen (Sigma, St. Louis, MO) in 0.05% (w/v) acetic acid at 4°C. The solution was then centrifuged at ~12,000 g at 4°C for 60 min, and its supernatant was filtered through a 0.45-μm Millipore®-HV durapore® membrane filter (Millipore, Bedford, MA). This final collagen solution (1 mg/mL) had a pH of 3.5. The AAG (Sigma) solution was prepared by dissolving the protein in 0.05% acetic acid, and similarly, had a final pH of 3.5.

Transmission Electron Microscopy

Copper indexed grids (600 mesh) were purchased (SPI, West Chester, PA) and were carbon-coated via methods previously described.[22] In short, carbon was first evaporated onto freshly cleaved mica and floated in Milli-Q deionized water where it was collected onto the copper grids. A drop of the FLS collagen fibril solution was placed onto the carbon-coated grid, and the excess amount was removed after 15 s by using filter paper. After the deposited sample was allowed to air dry, TEM and AFM images were obtained. The collagen fibrils were then negatively stained with 2% (w/v) solution of phosphotungstic acid (PTA), pH 7.0, at different time intervals, ranging from 30 s to 10 min, via methods previously described.[22] This

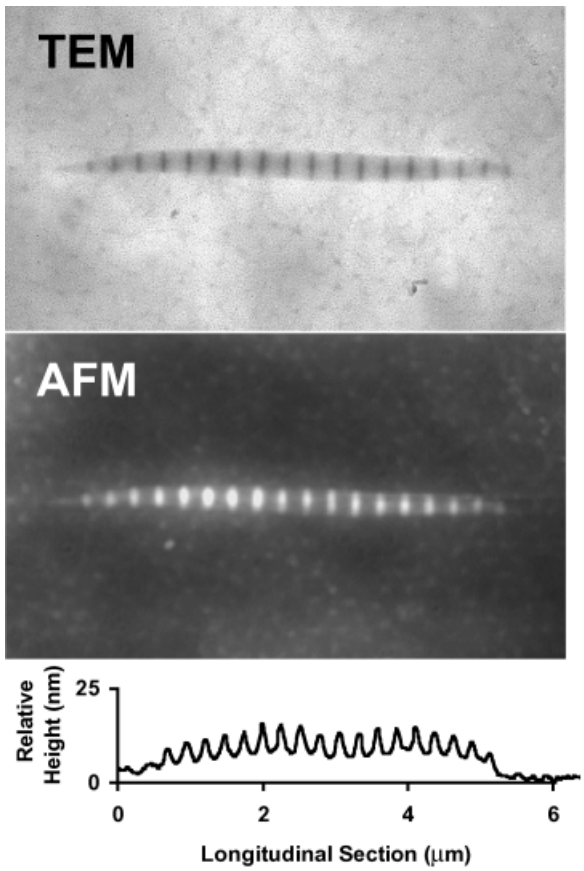

Fig. 1. TEM image (**top**) and AFM height image (**bottom**) of exactly the same area of FLS collagen fibril taken before negative staining with PTA. Image area: 3.0 μm × 6.0 μm; AFM height scale: 0 (dark) to 25 nm (light). A typical sectional measurement taken along the length of the fibril in the AFM height image is provided below the AFM height image. Note that negative staining is not required to achieve banding patterns observed under TEM.

method of obtaining TEM images of *unfixed* collagen constructs formed in vitro was achieved in the earliest work[2,13,14,41–43] to more recent accounts.[21,44–49] Excess stain was removed by touching the edge of the grid with filter paper. After drying, the same area was relocated by using the indices of the grid for both TEM and AFM imaging.[50] All TEM images were obtained with an Hitachi H-7000 Transmission Electron Microscope (Nissei Sangyo, Rexdale, ON) at 75 kV and 100 kV, at magnifications ranging from ×10,000 to ×100,000.

To determine the presence of PTA stain, energy dispersive X-ray (EDX) spectroscopy was performed on the same areas of FLS collagen fibrils after negative staining, noting the presence of spectral peaks signature to tungsten. Spectra were collected at magnifications ranging from ×10,000 to ×100,000 at 120 kV by using a Philips/FEI Tecnai 20 Transmission Electron Microscope (FEI Co., Hillsboro, OR) equipped with an EDAX Phoenix detector.

Atomic Force Microscopy

To image with the AFM exactly the same area of FLS collagen fibril observed under TEM, a holder was used to

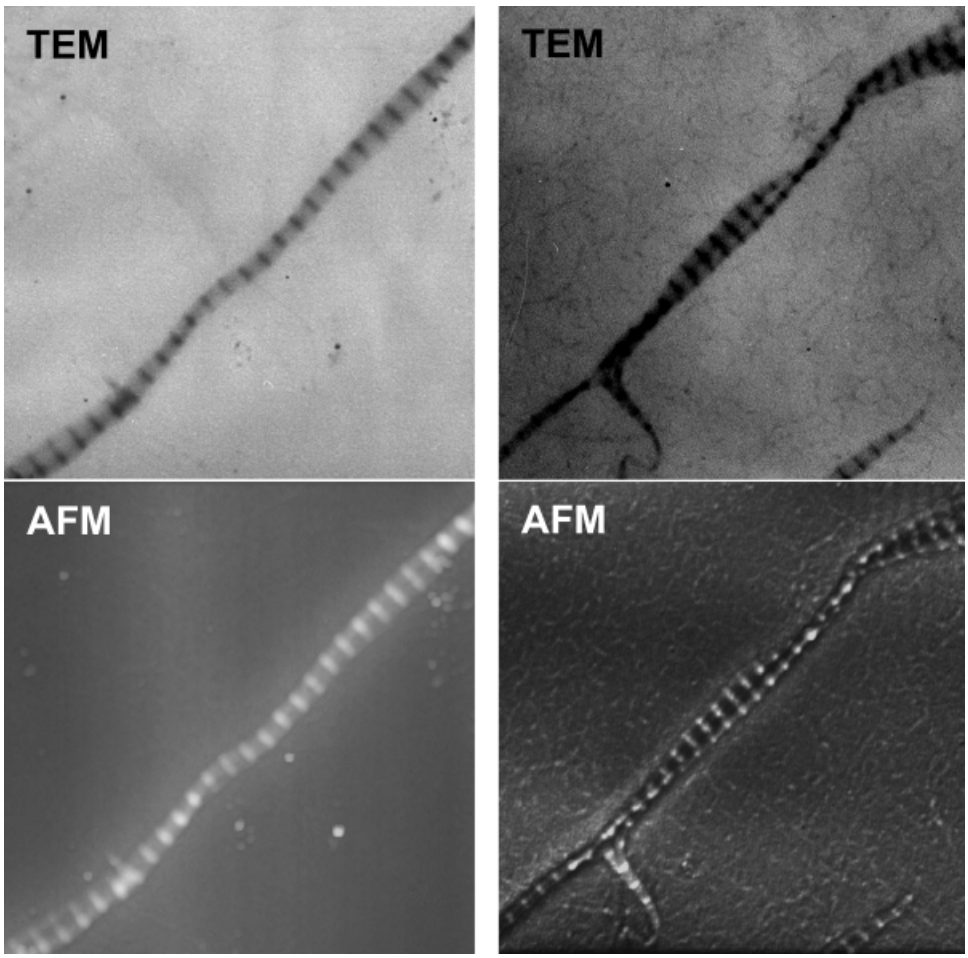

Fig. 2. Pairs of AFM and TEM images of exactly the same area of FLS collagen fibril sample taken before negative staining with PTA. **Left:** Image area: 5.0 μm × 5.0 μm; AFM height scale: 0 (dark) to 75 nm (light). **Right:** Image area: 6.0 μm × 6.0 μm; AFM height scale: 0 (dark) to 50 nm (light).

secure the carbon-coated TEM grid in place during AFM imaging.[21] All AFM imaging was performed in contact mode by using a Nanascope III instrument and silicon nitride tips of nominal spring constant 0.58 N/m (Digital Instruments, Santa Barbara, CA). AFM images were obtained at imaging speeds of 1–2 Hz, scanning 512 lines per image. Both deflection and height images were captured simultaneously.

All AFM measurements were taken from height images. For collagen fibrils imaged by AFM, two types of sectional measurements are commonly obtained from the AFM height image. Sectional measurements taken along the long axis of the fibril were used to determine the distance between adjacent protrusions and heights of protrusions relative to the interband region. Sectional measurements taken perpendicular to the long axis of the fibril at the protrusions were used to determine the height of these protrusions relative to the imaging substrate. Both types of sectional measurements were taken for each FLS fibril before and after negative staining with PTA, and these measurements were compared. All averaged values are reported with their corresponding standard error means.

RESULTS

AFM and TEM of Unstained FLS Collagen Fibrils

Figures 1 and 2 show both AFM and TEM images of the same area of FLS collagen fibrils obtained before negative staining with PTA. A representative longitudinal section taken from the AFM height image is also provided in Figure 1. On the basis of the analysis of these sectional measurements performed in real space and on the FT taken along several fibrils, a banding periodicity of ~265 nm and fibril heights of 100–250 nm were observed, which are in good comparison to previously reported measurements.[20] Note that a pronounced appearance of periodic dark bands along the longitudinal axis of the fibril is still observed by TEM, even though these fibrils were unstained.

AFM and TEM of Negatively Stained FLS Collagen Fibrils

Both AFM and TEM images were obtained for the same fibrils shown in Figures 1 and 2 after negative staining, as shown in Figures 3 and 4. These TEM images are similar

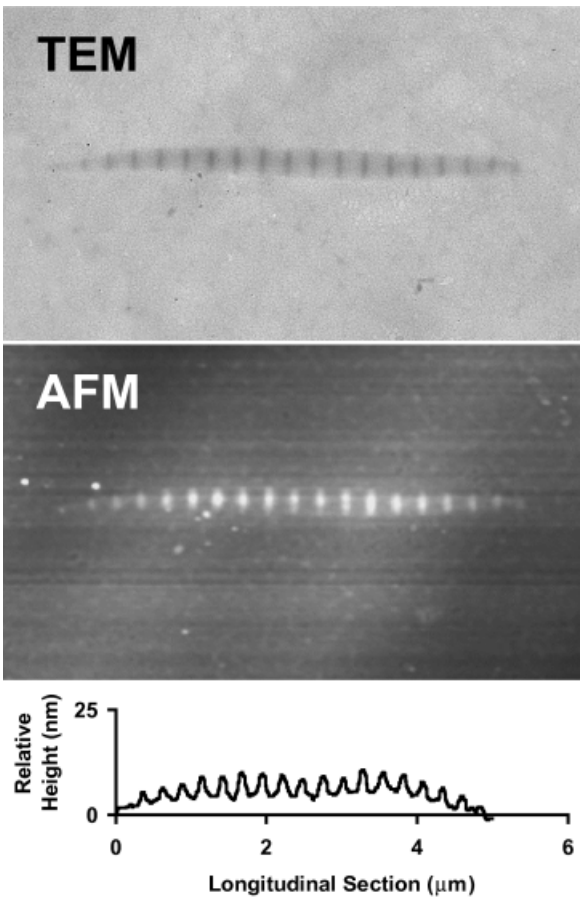

Fig. 3. TEM image (**top**) and AFM height image (**bottom**) of exactly the same area of FLS collagen fibril taken after negative staining with PTA. Image area: 3.0 μm × 6.0 μm; AFM height scale: 0 (dark) to 25 nm (light). A typical sectional measurement taken along the length of the fibril in the AFM height image is provided below the AFM height image. Note that the correspondence of protrusions revealed by AFM with dark bands observed by TEM does not change, even on negative staining.

to TEM images that were previously obtained of negatively PTA stained FLS collagen fibrils formed in vitro from type I collagen and AAG solutions.[2,21,41] Similar to those obtained before staining, several sectional measurements were obtained for each FLS fibril after negative staining. A representative longitudinal section taken from the AFM height image is also provided in Figure 3. In comparison with the values obtained before staining, the same measured banding periodicity and fibril heights were observed. On the basis of the correlated AFM and TEM images shown in Figures 3 and 4, the dark bands observed in TEM still correspond to protrusions along the fibril shown by AFM.

Stain Deposition Analysis

The presence of PTA stain in the negatively stained FLS collagen samples was investigated by electron dispersive X-ray (EDX) spectrometry and by comparing AFM sectional measurements obtained before and after staining. Figure 5(A) shows a representative EDX spectrum of these stained fibrils shown in Figures 3 and 4. The spectrum exhibits strong peaks signature to tungsten, indicating the presence of PTA stain in these samples. Figure 5(B) summarizes the decrease in the banding protrusion height with respect to the interband region (1.4 ± 0.7 nm) and carbon film (3.0 ± 0.7 nm). These decreases in height are statistically significant and indicate that the PTA deposited heavily onto the carbon film and preferentially in the interband regions of the fibril.

DISCUSSION

The present study shows that parallel AFM and TEM images can provide important complementary information in collagen fibril ultrastructural studies. Without the benefit of knowing the fibril's surface topography, it was suggested by Gross et al.[2] in their 1954 PNAS article on FLS collagen fibrils formed from type I collagen and AAG that "the major repeating dark bands of the FLS may be thick relative to the interband region because of the overlapping tropocollagen and because of the presence of dense spherodial material which is presumably composed of tropocollagen and acid glycoprotein." Our parallel AFM and TEM images obtained before staining confirms this idea: we have shown in Figures 1 and 2 that the periodic protrusions along the fibril revealed by AFM appear to be effective in scattering electrons and thus correspond directly to the dark bands observed under TEM. Moreover, these results show that negative staining is not required to achieve the banding patterns of dark and light regions observed in TEM images of FLS collagen fibrils.

It is unclear about what effect negative staining would have on the observed banding periodicity of dark and light bands. One suggestion is that the surface topography would dictate the manner in which the stain could accumulate along the bulk fibril.[3] Thus, the idea is that the banding pattern would become inverted as the area between protrusions (the interband region) would collect greater amounts of stain and register as the darker band in comparison to the protrusions. Alternatively, the fibril could be stained while the banding contrast remains unchanged. To investigate these claims, the same area of FLS collagen fibril examined before staining was reexamined after negative staining by parallel AFM and TEM.

After negative staining with PTA, the same FLS fibrils shown in Figures 1 and 2 were relocated on the indexed TEM grids, and both AFM and TEM images were obtained, as shown in Figures 3 and 4. Although these fibrils have been negatively stained, the repeating dark bands seen under TEM still correspond to the periodic protrusions along the FLS collagen fibril shown by AFM. To investigate the staining of these fibrils with PTA, we performed two independent quantitative measurements, each relying on a salient feature of one of the two microscopy techniques.

In TEM, energy dispersive X-ray (EDX) spectrometry can provide information on the elemental composition of a sample. As shown in the representative EDX spectrum in Figure 5(A), strong peaks characteristic of tungsten are registered for these stained samples, indicating the presence of PTA stain.

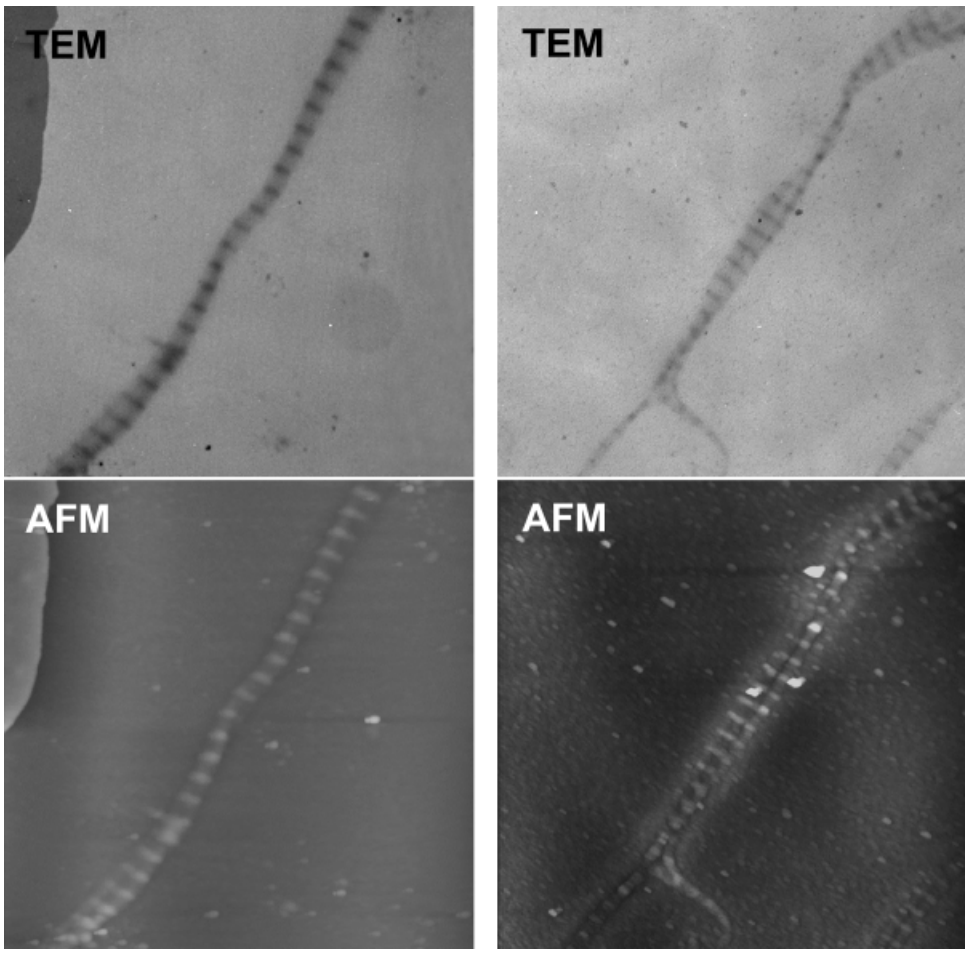

Fig. 4. Pairs of AFM and TEM images of exactly the same area of FLS collagen fibril sample (shown in Fig. 2) taken after negative staining with PTA. **Left:** Image area: 5.0 μm × 5.0 μm; AFM height scale: 0 (dark) to 75 nm (light). **Right:** Image area: 6.0 μm × 6.0 μm; AFM height scale: 0 (dark) to 50 nm (light).

In AFM, the height of the protrusions with respect to the interband region and carbon film can be obtained from sectional measurements. If the surface topography dictates the manner in which negative stain accumulates, negative stain should preferentially accumulate in the interband region. Therefore, there should be a decrease in protrusion height with respect to the interband region on negative staining. Moreover, a decrease in protrusion height should be observed with respect to the carbon film if stain accumulation around the fibril occurs. As illustrated Figure 5(B), a decrease in protrusion height with respect to the interband region and carbon film occurred on negative staining. Note that these values of height changes are not absolute but do suggest negative PTA stain deposition.

Therefore, through parallel AFM and TEM of the exact same sample area, we have confirmed the proposal made by Gross, Highberger, and Schmitt and have shown that the periodic dark bands along FLS collagen fibrils observed under TEM correspond directly to the periodic protrusions revealed by AFM, irrespective of negative staining. The observation of banding by TEM even without negative staining and the measurements that showed stain deposition on the fibril surface in negatively stained samples imply that stain penetration into the fibril and deposition into empty spaces is not an important factor. The contrast of dark and light regions observed under TEM along these FLS collagen fibrils is due to the ability of the protrusions to scatter electrons and register as the darker bands in TEM. Thus, although we cannot rule out the presence of gap zones, we have shown that there is no need to invoke it in a model for FLS collagen fibrils. Noting that the banding period (~265 nm) is slightly less than the monomer length (~280–300 nm), we can conjecture, along with Gross et al.,[2] that banding in FLS collagen fibrils is due to overlap of the monomers and possibly the location of AAG within the fibrils.

CONCLUSIONS

A parallel AFM-TEM approach has been used to investigate the ultrastructure of FLS collagen fibrils. By obtaining both AFM and TEM images of exactly the same area of FLS collagen fibrils, it has been shown that the periodic dark bands along the length the fibril observed in TEM images correspond directly to the periodic protrusions of material elucidated by AFM, irrespective of negative staining with PTA. The presence of more material, possibly

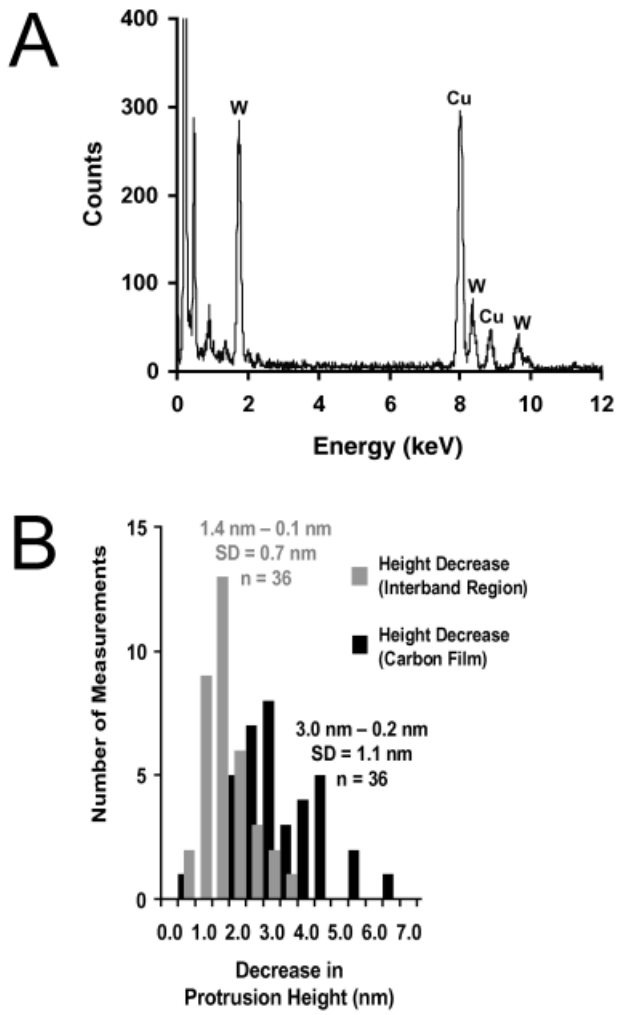

Fig. 5. **A:** Representative EDX spectrum obtained from the PTA stained FLS collagen samples shown in Figures 3 and 4. This particular spectrum was obtained at a magnification of ×89,000. Strong signature tungsten peaks are observed, confirming the presence of PTA in these negatively stained samples. Note the signature copper peaks from the copper TEM grids. **B:** Histogram showing the decrease in height of the banding protrusion with respect to the interband region (gray) and carbon film (black) after negative staining. This decrease in height can be attributed to the deposition of stain along the fibril on the carbon film. Note that the reported errors are standard error means.

AAG and/or telopeptides, in these elevated regions is sufficient to scatter electrons and register as dark bands in TEM. On the basis of the correlated AFM and TEM images, there is no need to invoke gap regions to explain the banding periodicity observed of FLS collagen fibrils formed in vitro from type I collagen and AAG solutions. Rather, the much earlier surmise of Gross, Highberger, and Schmitt is more appropriate.

ACKNOWLEDGMENTS

The authors thank R. Villadiego for his TEM technical assistance, D. Holmyard for his help with EDX spectroscopy, and J. K. Rainey and M. F. Paige for their helpful discussions. The continuing support of the Natural Science and Engineering Research Council (NSERC) of Canada is gratefully acknowledged.

REFERENCES

1. Nimni ME. Collagen. Boca Raton, FL: CRC Press; 1988.
2. Gross J, Highberger JH, Schmitt FO. Collagen structures considered as states of aggregation of a kinetic unit: the tropocollagen particle. Proc Natl Acad Sci USA 1954;40:679–688.
3. Paige MF, Rainey JK, Goh MC. A study of fibrous long spacing collagen ultrastructure and assembly by atomic force microscopy. Micron 2001;32:341–353.
4. Morris CJ, Bradby GV, Walton KW. Fibrous long-spacing collagen in human atherosclerosis. Atherosclerosis 1978;31:345–354.
5. Nakanishi I, Masuda S, Kitamura T, Moriizumi T, Kajikawa K. Distribution of fibrous long-spacing fibers in normal and pathological lymph nodes. Acta Pathol Jpn 1981;31:733–745.
6. Kamiyama R. Fibrous long spacing-like fibers in the bone marrow of myloproliferative disorder. Virchows Arch B Cell Pathol Incl Mol Pathol 1982;39:285–291.
7. Slavin RE, Swedo JL, Brandes D, Gonzalez-Vitale JC, Osornio-Vargas A. Extrapulmonary silicosis: a clinical, morphologic, and ultrastructural study. Hum Pathol 1985;16:393–412.
8. Kadler KE, Holmes DF, Trotter JA, Chapman JA. Collagen fibril formation. Biochem J 1996;316:1–11.
9. Holmes DF, Graham HK, Trotter JA, Kadler KE. STEM/TEM studies of collagen fibril assembly. Micron 2001;32:273–285.
10. Petruska JA, Hodge AJ. Recent studies with the electron microscope on ordered aggregates of the tropocollagen molecule. In: Ramachandran GN, editor. Aspects of protein structure. New York: Academic Press; 1963. p. 289–300.
11. Petruska JA, Hodge AJ. A subunit model for the tropocollagen macromolecule. Proc Natl Acad Sci USA 1964;51:871–876.
12. Chapman JA, Armitage PM. An analysis of fibrous long spacing forms of collagen. Connect Tiss Res 1972;1:31–37.
13. Gross J, Highberger JH, Schmitt FO. Extraction of collagen from connective tissue by neutral salt solutions. Proc Natl Acad Sci USA 1955;41:1–7.
14. Highberger JF, Gross J, Schmitt FO. Electron microscope observations of certain fibrous structures obtained from connective tissue extracts. J Am Chem Soc 1950;72:3321–3322.
15. Ghadially FN. Ultrastructural pathology of the cell and matrix. London: Butterworths; 1988. p. 698–705.
16. Chernoff EAG, Chernoff DA. Atomic force microscope images of collagen fibres. J Vacuum Sci Technol 1992;A10:596–599.
17. Baselt DR, Revel J-P, Baldeschwieler JD. Subfibrillar structure of type I collagen observed by atomic force microscopy. Biophys J 1993;65:2644–2655.
18. Revenko I, Sommer F, Minh DT, Garrone R, Franc JM. Atomic force microscopy study of the collagen fibre structure. Biol Cell 1994;80:67–69.
19. Gale M, Pollanen MS, Markiewicz P, Goh MC. Sequential assembly of collagen revealed by atomic force microscopy. Biophys J 1995;68:2124–2128.
20. Paige MF, Rainey JK, Goh MC. Fibrous long spacing collagen ultrastructure elucidated by atomic force microscopy. Biophys J 1998;74:3211–3216.
21. Lin AC, Goh MC. A novel sample holder allowing atomic force microscopy on transmission electron microscopy specimen grids: repetitive, direct correlation between AFM and TEM images. J Microsc 2002;205:205–208.
22. Gathercole LJ, Miles MJ, McMaster TJ, Holmes DF. Scanning probe microscopy of collagen I and pN-collagen I assemblies and the relevance to scanning tunnelling microscopy contrast generation in protein. J Chem Soc Faraday Trans 1993;89:2589–2594.
23. Adachi E, Katsumata O, Yamashina S, Prockop DJ, Fertala A. Collagen II containing a Cys substitution for Arg-alpha 1-519. Analysis by atomic force microscopy demonstrates that mutated monomers alter the topography of the surface of collagen II fibrils. Matrix Biol 1999;18:189–196.
24. Arakawa H, Umemura K, Ikai A. Protein images obtained by STM, AFM and TEM. Nature 1992;358:171–173.
25. Devaud G, Furcinitti PS, Fleming JC, Lyon MK, Douglas K. Direct observation of defect structure in protein crystals by atomic force and transmission electron microscopy. Biophys J 1992;63:630–638.
26. Ikai A, Imai K, Yoshimura K, Tomitori M, Nishikawa O, Kokawa R, Kobayashi M, Yamamoto M. Scanning-tunneling-microscopy atomic-force microscopy studies of bacteriophage-T4 and its tail fibers. J Vacuum Sci Technol B 1994;12:1478–1481.

27. Braet F, De Zanger R, Kalle W, Raap A, Tanke H, Wisse E. Comparative scanning, transmission and atomic force microscopy of the microtubular cytoskeleton in fenestrated liver endothelial cells. Scann Microsc Suppl 1996;10:225–235.
28. Valle M, Valpuesta JM, Carrascosa JL, Tamayo J, Garcia R. The interaction of DNA with bacteriophage phi 29 connector: a study by AFM and TEM. J Struct Biol 1996;116:390–398.
29. Jurvelin JS, Muller DJ, Wong M, Studer D, Engel A, Hunziker EB. Surface and subsurface morphology of bovine humeral articular cartilage as assessed by atomic force and transmission electron microscopy. J Struct Biol 1996;117:45–54.
30. Yoshida T, Wakiyama M, Yazaki K, Miura K. Transmission electron and atomic force microscopic observation of polysomes on carbon-coated grids prepared by surface spreading. J Electron Microsc 1997;46:503–506.
31. Wiesmann HP, Chi L, Stratmann U, Plate U, Fuchs H, Joos U, Hohling HJ. Sutural mineralization of rat calvaria characterized by atomic-force microscopy and transmission electron microscopy. Cell Tissue Res 1998;294:93–97.
32. Nag K, Munro JG, Hearn SA, Rasmusson J, Petersen NO, Possmayer F. Correlated atomic force and transmission electron microscopy of nanotubular structures in pulmonary surfactant. J Struct Biol 1999;126:1–15.
33. Keller D. Reconstruction of STM and AFM images distorted by finite-size tips. Surf Sci 1991;253:353–364.
34. Mulvaney P, Giersig M. Imaging nanosized gold colloids by atomic force microscopy: a direct comparison with transmission electron microscopy. J Chem Soc Faraday T 1996;92:3137–3143.
35. Posfai M, Xu HF, Anderson JR, Buseck PR. Wet and dry sizes of atmospheric aerosol particles: an AFM-TEM study. Geophys Res Lett 1998;25:1907–1910.
36. Pfau A, Janke A, Heckmann W. Determination of the bulk structure of technical multiphase polymer systems with AFM: comparative AFM and TEM investigation. Surf Interface Anal 1999;27:410–417.
37. Thomann Y, Thomann R, Bar G, Ganter M, MacHutta B, Mulhaupt R. Combined ultramicrotomy for AFM and TEM using a novel sample holder. J Microsc 1999;195:161–163.
38. Visconti P, Huang D, Reshchikov MA, Yun F, King T, Baski AA, Cingolani R, Litton CW, Jasinski J, Liliental-Weber Z, et al. Investigation of defects and polarity in GaN using hot wet etching, atomic force and transmission electron microscopy and convergent beam electron diffraction. Phys Status Solidi B 2001;228:513–517.
39. He L, Siewenie JE. Cryogenic processing of thin metal films. Surface Coatings Technol 2002;150:76–79.
40. Hornyak GL, Peschel S, Sawitowski T, Schmid G. TEM, STM and AFM as tools to study clusters and colloids. Micron 1998;29:183–190.
41. Highberger JH, Gross J, Schmitt FO. The interaction of mucoprotein with soluble collagen: an electron microscope study. Proc Natl Acad Sci USA 1951;37:286–291.
42. Cox RW, Grant RA, Horne RW. The structure and assembly of collagen fibrils. I. Native-collagen fibrils and their formation from tropocollagen. J R Microsc Soc 1967;87:123–142.
43. Grant RA, Cox RW, Horne RW. The structure and assembly of collagen fibrils. II. An electron-microscope study of cross-linked collagen. J R Microsc Soc 1967;87:143–155.
44. Lilja S, Barrach HJ. An electron microscopical study of the influence of different glycosaminoglycans on the fibrillogenesis of collagen type I and II in vitro. Virchows Arch A Pathol Anat Histol 1981;390:325–338.
45. Kuhn K. Segment-long-spacing crystallites, a powerful tool in collagen research. Coll Relat Res 1982;2:61–80.
46. Mallinger R, Schmut O. In vitro fibrillogenesis of interstitial collagens: electron microscopical studies of long-spacing forms induced by chondroitin sulfate. J Submicrosc Cytol 1985;17:177–182.
47. Mallinger R, Schmut O. Reaggregation behavior of different types of collagen in vitro: variations in the occurrence and structure of dimeric segment long-spacing collagen. J Ultrastruct Mol Struct Res 1988;98:11–18.
48. Kobayashi K, Niwa J, Hoshino T, Nagatani T. Electron microscopic visualization of collagen aggregates without chemical staining. J Electron Microsc (Tokyo) 1992;41:235–241.
49. Fujita Y, Kobayashi K, Hoshino T. Atomic force microscopy of collagen molecules. Surface morphology of segment-long-spacing (SLS) crystallites of collagen. J Electron Microsc (Tokyo) 1997;46:321–326.
50. Markiewicz P, Goh MC. Identifying locations on a substrate for the repeated positioning of AFM samples. Ultramicroscopy 1997;68:215–221.